

Background

Gamma delta ($\gamma\delta$) T cells are a unique subset of lymphocytes that possess innate and adaptive immune functions. Unlike conventional $\alpha\beta$ T cells, $\gamma\delta$ T cells recognize antigens in an MHC-independent manner. This allows them to detect a wide range of stress-induced ligands that are commonly expressed on tumor cells. This property makes $\gamma\delta$ T cells particularly attractive for cancer immunotherapy, especially in cases where tumors evade immune surveillance by downregulating MHC molecules. Recent advances in cellular engineering have made it possible to generate $\gamma\delta$ T cells that express chimeric antigen receptors (CARs), which combines their natural tumor-recognition capabilities with the targeted specificity of CARs. $\gamma\delta$ CAR T cells offer several advantages over $\alpha\beta$ CAR T cells, including lower graft-versus-host disease risk, suitability for allogeneic applications ("out-of-the-shelf"), and enhanced solid tumor infiltration due to tissue-homing properties. These properties provide a strong rationale for investigating $\gamma\delta$ CAR T cells as a novel cancer therapy approach and underscore the importance of continued optimization to realize their full therapeutic potential.

Method

Generation and Characterization of $\gamma\delta$ and $\alpha\beta$ CAR T Cells

T cells were isolated from healthy human donors and enriched for $\gamma\delta$ T cells by selective depletion of $\alpha\beta$ T cells. The enriched $\gamma\delta$ T cells were activated, and two days after activation, the lentiviral CAR construct was added. Transduced $\gamma\delta$ CAR T cells were subsequently expanded for an additional two weeks under standard culture conditions. In parallel, $\alpha\beta$ CAR T cells were generated from the same donors using an analogous workflow, enabling direct donor-matched comparisons between $\gamma\delta$ and $\alpha\beta$ CAR T cell products.

The resulting CAR T cells were characterized by flow cytometry for surface CAR expression. Functional activity was assessed by measuring degranulation upon target engagement using CD107a staining. Cytotoxic activity was evaluated *in vitro* using a bioluminescence based-killing assay with luciferase-expressing NALM-6 target cells, and cytokine secretion was quantified by measuring IFN- γ and TNF levels following co-culture.

In Vivo Efficacy Studies

In vivo antitumor efficacy was assessed using a disseminated xenograft model with luciferase-expressing NALM-6 (NALM-6_Luc) cells. One million NALM-6_Luc cells were injected intravenously into NXG mice (Janvier). Mice received repeated supplementation with human IL-15 (1 μ g per mouse) administered every 3–4 days to support CAR T cell persistence. Tumor growth was monitored longitudinally by bioluminescence imaging using an IVIS[®] Lumina III imaging system (Revvity). The antitumor activity of standard $\gamma\delta$ CAR T cells was directly compared with donor-matched $\alpha\beta$ CAR T cells in this model.

Summary

- Highly pure $\gamma\delta$ and $\alpha\beta$ CAR T cell products with robust and uniform CAR expression were successfully generated.
- Despite similar degranulation, $\alpha\beta$ CAR T cells exhibited slower cytotoxic killing capacity, while producing higher levels of cytokines.
- Incorporation of the cytoplasmic CD3 ϵ domain resulted in slightly reduced killing activity at shorter times, associated with lower cytokine secretion
- The NALM-6 model proved well-suited for CAR T cell evaluation due to its high engraftment rate and low tumor heterogeneity.
- In vivo* efficacy studies revealed superior antitumor activity of $\alpha\beta$ CAR T cells compared with $\gamma\delta$ CAR T cells. Still, $\gamma\delta$ CAR T cells might be an attractive out-of-the-shelf alternative for patients with limited options.

Generation and characterization of CAR T cells

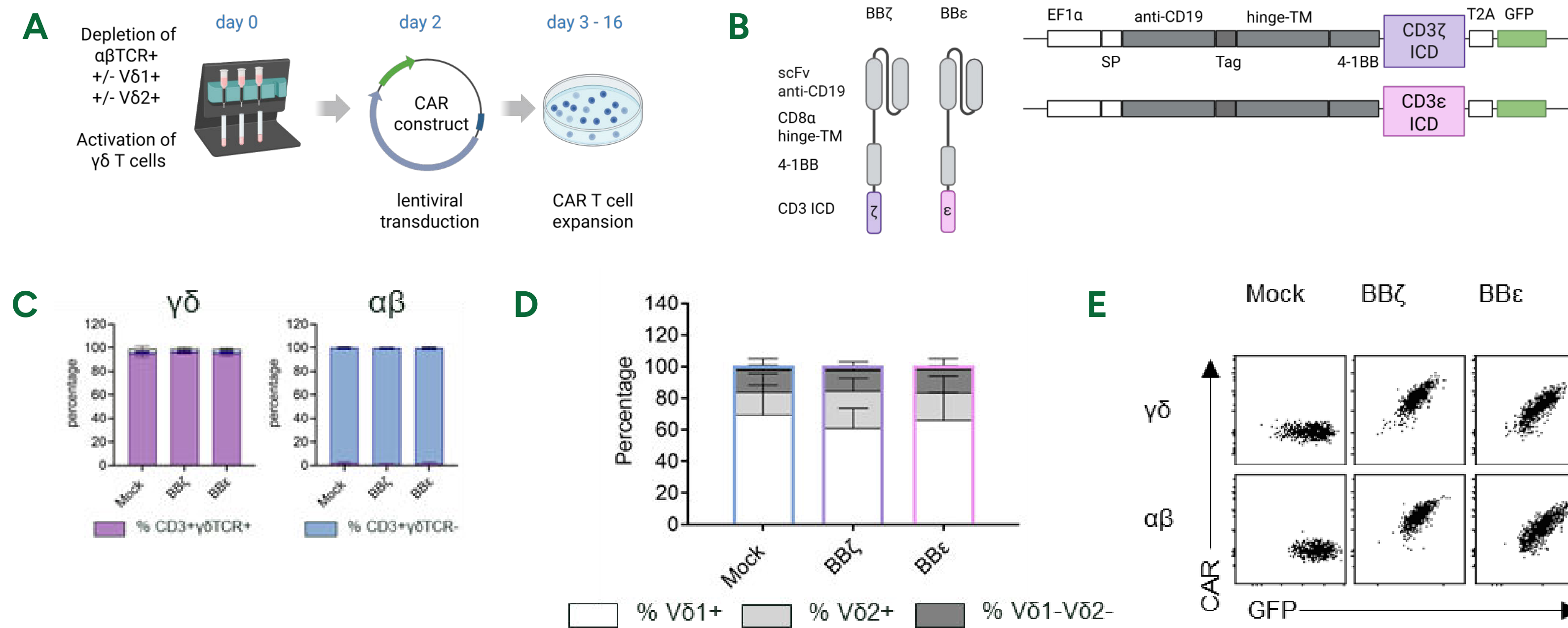


Figure 1: (A) Schematic overview of $\gamma\delta$ CAR T cell expansion protocols. (B) Schematic representation of the chimeric antigen receptor (CAR) constructs used in this study. (C) Proportions of CD3⁺ and $\gamma\delta$ TCR⁺ cells after sorting, assessed by flow cytometry (n = 3–5). (D) Frequencies of V δ 1⁺, V δ 2⁺, and V δ 1⁺V δ 2⁻ $\gamma\delta$ T cell subsets determined by flow cytometry; data pooled from 3–5 independent experiments. (E) Representative flow cytometry plots from a single donor showing GFP versus CAR expression for each CAR construct.

Functional *in vitro* evaluation of CAR T cells

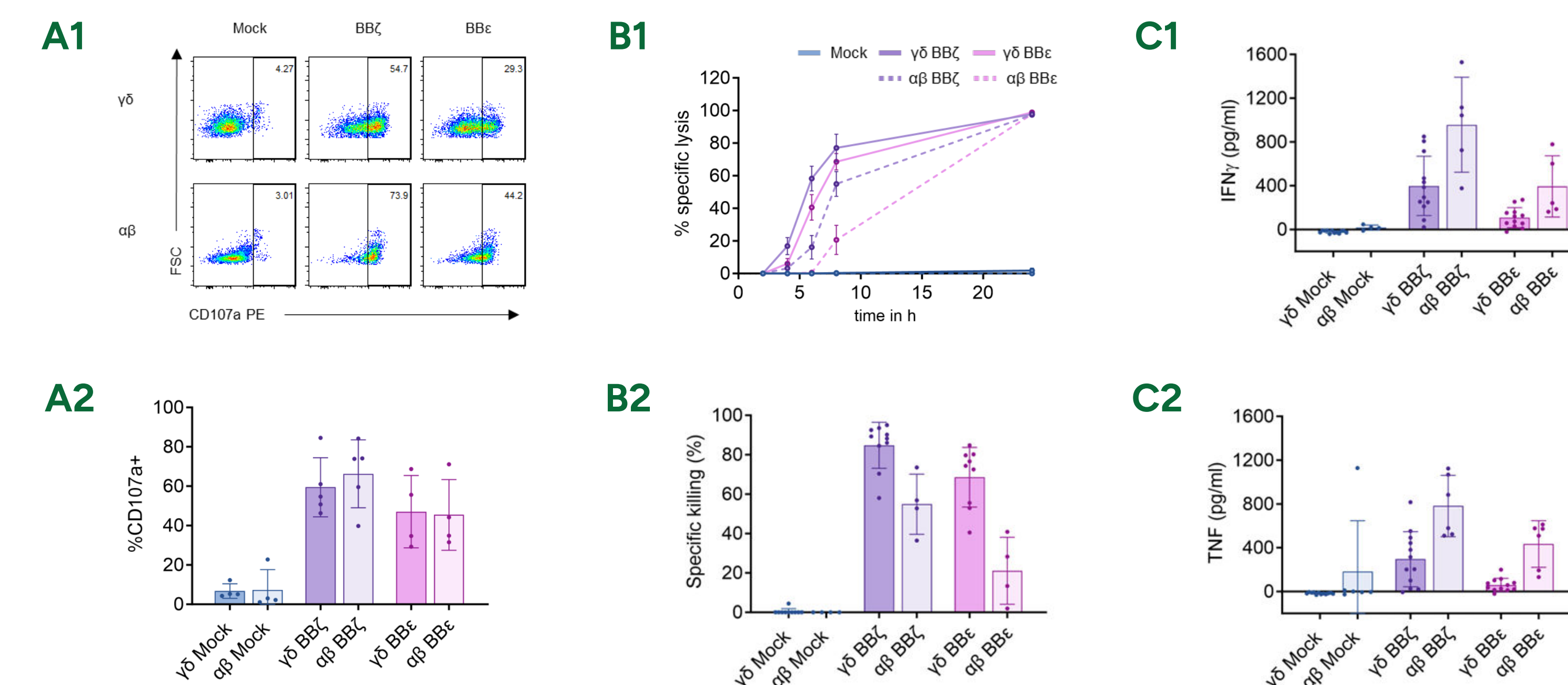


Figure 2: (A1) Representative flow cytometry plots of CD107a expression on CAR T cells after a 4-h co-culture with CD19⁺ NALM-6 cells at an E:T ratio of 1:1. (A2) Frequency of CD107a⁺ CAR T cells. (mean \pm SD, n = 3–4 donors; each dot represents one donor) (B1) Specific lysis of NALM-6_Luc target cells over time. (B2) Quantification of specific lysis after 8 h of co-culture. Data are presented as mean \pm SD from n = 3–4 independent donors. (C) CAR T cells were co-cultured with CD19⁺ NALM-6 tumor cells at an effector-to-target (E:T) ratio of 1:1 for 24 h. Secretion of IFN- γ (C1) and TNF (C2) was quantified by ELISA. Data are shown as mean \pm SD from 4–5 healthy donors, with each dot representing one donor.

In vivo efficacy study

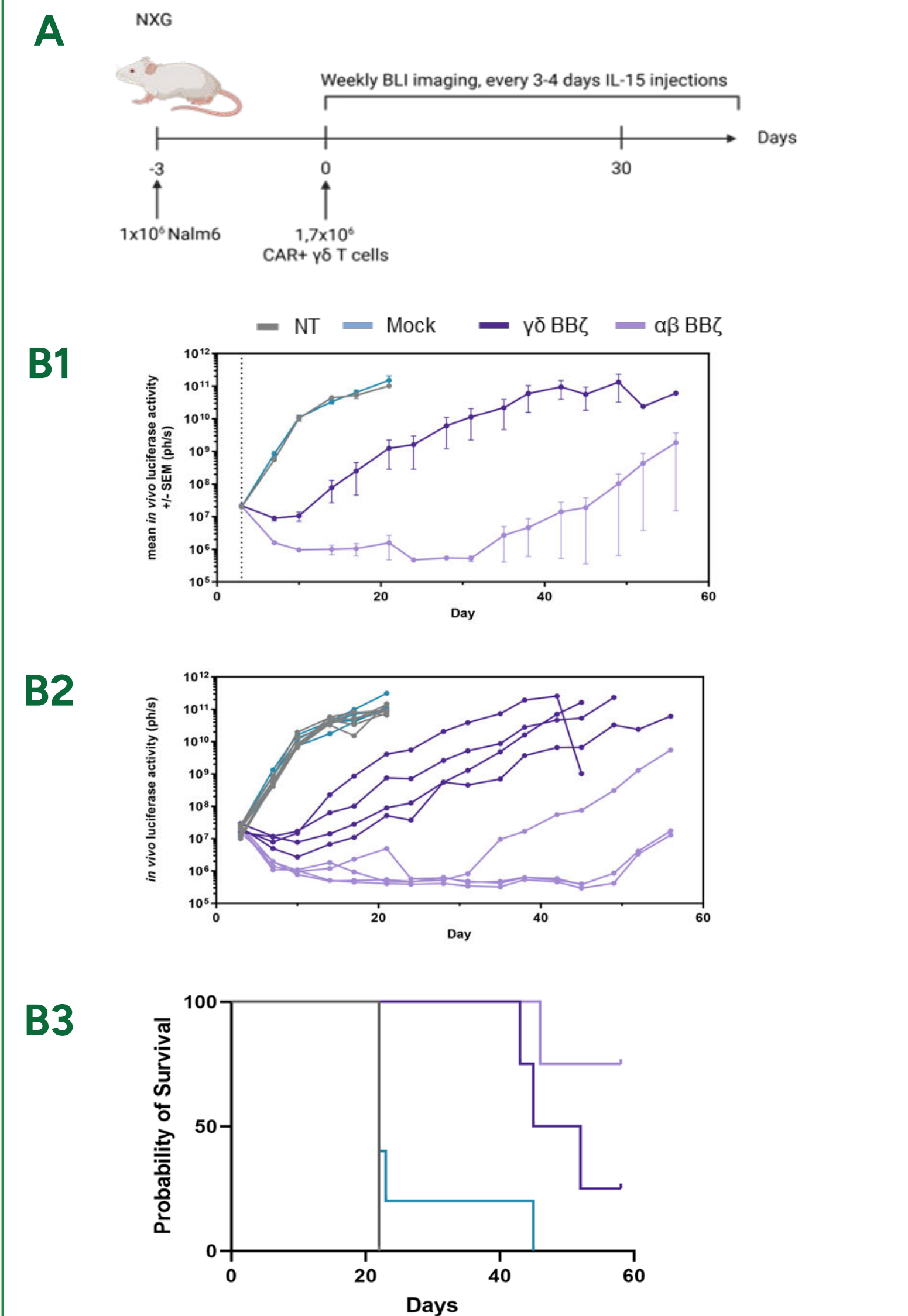


Figure 3: (A) Schematic overview of the *in vivo* efficacy study. One million NALM-6_Luc cells were injected intravenously into NXG mice (Janvier) on day -3. CAR T cells (1.7 million/mouse) were administered on day 0. To support CAR T cell persistence, mice received human IL-15 (1 μ g per mouse) every 3–4 days. (B) Tumor progression in untreated control mice, mock-transduced $\gamma\delta$ T cell-treated mice, $\gamma\delta$ BBz CAR T cell-treated mice, and $\alpha\beta$ BBz CAR T cell-treated mice was monitored by bioluminescence imaging using an IVIS[®] Lumina III system (Revvity). (B1) Mean *in vivo* bioluminescence signal over time, shown as mean \pm SEM for each treatment group. (B2) Individual bioluminescence kinetics of single mice, illustrating inter-animal variability in tumor progression. (B3) Kaplan–Meier survival curves comparing overall survival across the different treatment groups.

Contact

Holger Weber, PhD

Reaction Biology Europe +49-151-2400023

Engesserstr. 4

79108 Freiburg, Germany

Holger.Weber@reactionbiology.com

www.reactionbiology.com